

Optical Spectrum of Antiferromagnetic  $\text{Cr}_2\text{O}_3$ 

J. P. VAN DER ZIEL

*Bell Telephone Laboratories, Murray Hill, New Jersey*

(Received 20 March 1967; revised manuscript received 12 May 1967)

The sharp absorption spectrum of antiferromagnetic  $\text{Cr}_2\text{O}_3$  is investigated. The molecular-field approximation to the exchange interaction is shown to be inapplicable to the  ${}^2E$  states. A modified exchange interaction is introduced via an effective Hamiltonian, and the resulting transitions are interpreted in terms of exciton theory. Reasonable agreement with experiment is found. With a magnetic field parallel to the  $c$  axis, a new line not present in zero field is observed. This absorption is explained by the exciton theory. The  $3.75\text{-cm}^{-1}$  separation between the satellite line and the line from which it borrows its intensity is a Davydov splitting. No electric field effect for fields up to  $100\text{ kV/cm}$  is found. Finally, the low-temperature fluorescence spectrum is discussed.

## I. INTRODUCTION

IN a recent letter, the optical absorption spectrum resulting from the  ${}^4A_2$  to  ${}^2E$  transitions of  $\text{Cr}^{2+}$  in antiferromagnetic  $\text{Cr}_2\text{O}_3$  was discussed.<sup>1</sup> It was found that the molecular-field approximation does not properly account for the observed splittings of the  ${}^2E$  state. We discuss here the nature of the exchange of the excited state and present a more detailed discussion of the experimental results.

As found by McClure,<sup>2</sup> the main features of the spectrum are similar to chromium-doped  $\text{Al}_2\text{O}_3$ . The absorption lines were initially investigated at high resolution by Wickersheim,<sup>3</sup> and the Zeeman effect was measured by Stager.<sup>4</sup> We have essentially repeated their experiment, but have a significantly different interpretation of the results. In  $\text{Cr}_2\text{O}_3$  the optical absorption is best described in terms of Frenkel exciton theory.<sup>5,6</sup> In Sec. II the exciton spectrum resulting from the  ${}^4A_2$  to  ${}^2E$  single-ion transitions is derived. This is done first using the molecular-field approximation for the ground and excited states. It is the lowest-order approximation to the isotropic exchange interaction  $J_{12}\mathbf{S}_1 \cdot \mathbf{S}_2$ . Here  $\mathbf{S}_1$  and  $\mathbf{S}_2$  are the spins on ions 1 and 2, respectively. Van Vleck<sup>7</sup> has shown, however, that the isotropic exchange is only valid in certain limited situations. It is warranted when the ion has a half-filled shell, and when the ion is in its state of maximum multiplicity. This is the case when the chromium ions are in the  ${}^4A_2$  ground state, but does not apply for the exchange interaction between an ion in the  ${}^2E$  state and the  ${}^4A_2$  state, even though these states

arise from the same  $t^3$  strong-field configuration. It is not surprising that the results of the molecular-field approximation fail to agree with the experimental results shown in Table I. An exchange interaction capable of explaining the four transitions given in Table I is then introduced. The experimental absorption data are compared with theory in Sec. III, and the fluorescence from  $\text{Cr}_2\text{O}_3$  is discussed in Sec. IV.

II. EXCITONS IN  $\text{Cr}_2\text{O}_3$ 

The theory of excitons in antiferromagnetic crystals has received an extensive discussion by Loudon.<sup>8</sup> His work is an extension of the exciton theory of molecular

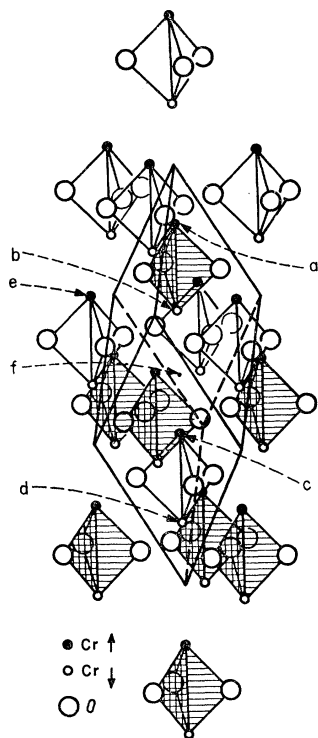
TABLE I. Absorption data for the sharp lines at  $4.2^\circ\text{K}$ .

Line	$\nu\text{ cm}^{-1}$	$\int\sigma_{\perp}d\nu$ ( $10^{-20}\text{ cm}$ )	$\int\sigma_{\parallel}d\nu$ ( $10^{-20}\text{ cm}$ )
1	13 747.0	11.2	0.3
2	13 769.5	0.9	5.0
3	13 909.5	0.6	3.2
4	13 931.4	6.3	<0.2

crystals.<sup>5,6</sup> Only the features of the theory directly applicable to the present case will be reviewed here. The fundamental principle is that stationary states of the crystal belong to the irreducible representations of the crystal space group. The crystal ground state transforms as the  $\Gamma_1^+$  representation. The exciton functions corresponding to  $\mathbf{k}=0$  of the Brillouin zone, which are important in optical absorption, transform as representations of the factor group of the space group.

The number and symmetry of the excitons resulting from a particular single-ion transition are found using group theory. In antiferromagnets the irreducible representations of the *site* wave functions which have the same energy, but are located on opposite sublattices are Kramers conjugates. The ground-state-site wave function does not transform as the totally symmetric representation. An ion is excited from its ground state  $|g\rangle$  to the state  $|e\rangle$  by the site transition operator

<sup>8</sup> R. Loudon (unpublished).<sup>1</sup> J. P. van der Ziel, Phys. Rev. Letters **18**, 237 (1967).<sup>2</sup> D. S. McClure, J. Chem. Phys. **38**, 2289 (1963).<sup>3</sup> K. A. Wickersheim, J. Appl. Phys. **34**, 1224 (1963).<sup>4</sup> C. V. Stager, J. Appl. Phys. **34**, 1232 (1963).<sup>5</sup> A. S. Davydov, *Theory of Molecular Excitons* (McGraw-Hill Book Company, Inc., New York, 1962).<sup>6</sup> The theory of Frenkel excitons has been reviewed by D. S. McClure [Solid State Phys. **8**, 1 (1959)] and by R. S. Knox [Solid State Phys. Suppl. **5**, 1 (1963)].<sup>7</sup> J. H. Van Vleck, Rev. Univ. Nac. Tucuman, Ser. A: **14**, 189 (1962). Anisotropic exchange interactions observed in the spectra of the rare-earth garnets have been discussed by K. A. Wickersheim and R. L. White [Phys. Rev. Letters **8**, 483 (1962)], and P. M. Levy [Phys. Rev. **135**, A155 (1964)].

FIG. 1. The structure of  $\text{Cr}_2\text{O}_3$ .

$|e\rangle\langle g|$ . The  $\mathbf{k}=0$  excitons are formed from the appropriate linear combination of single-ion excitations. The character of the exciton transition operator for the symmetry operation  $R$ , in terms of the character of the site  $\chi^{s\cdot g}(R)$ , is obtained by combining the transition operator characters of all the sites in a unit cell according to

$$X_j(R) = \sum_a \sigma_a(R) \chi_j^{s\cdot g}(R),$$

$$\begin{aligned} \sigma_a &= 1 && \text{if } R \text{ is an operation of the } a\text{th site group,} \\ &= 0 && \text{otherwise.} \end{aligned} \quad (1)$$

The reduction of  $X_j(R)$  into the irreducible representations of the factor group of the space group gives the exciton levels resulting from a single-ion transition having a final energy  $E_j$ .<sup>9</sup> Since the ground state is totally symmetric, these representatives also give the symmetry of the exciton states.

$\text{Cr}_2\text{O}_3$  has the corundum structure shown in Fig. 1.<sup>10</sup> The lattice may be considered as an array of antiferromagnetically ordered  $\text{Cr}_2\text{O}_3$  molecules with a unit cell containing two molecules.<sup>11</sup> The chromiums between the same two planes of oxygens, for example ions  $b$

<sup>9</sup> H. Winston, *J. Chem. Phys.* **19**, 156 (1951).

<sup>10</sup> P. P. Ewald and C. Hermann, *Z. Krist.* **1**, 240 (1931); S. Geschwind and J. P. Remeika, *Phys. Rev.* **122**, 757 (1961).

<sup>11</sup> B. N. Brockhouse, *J. Chem. Phys.* **21**, 961 (1953); D. E. Cox, W. J. Takei, and G. Shirane, *Phys. Chem. Solids* **24**, 405 (1963).

and  $e$ , are related by inversion followed by inversion of the spin. Although not clearly shown in Fig. 1, chromiums are opposite sides of an oxygen plane, such as  $a$  and  $b$ , are inequivalent as a result of a small unequal rotation of the oxygen triangles from the neighboring  $\text{Cr}_2\text{O}_3$  molecules around the chromium ion, thus reducing the site symmetry from  $C_{3v}$  to  $C_3=3$ . The point  $f$  at the center of the cell has symmetry  $C_{3i}=\bar{3}$ . In the paramagnetic phase the crystal symmetry is  $D_{3d}^6=R\bar{3}c'$ . The time reversal operator  $K$  denoted in the space group symbol by  $1'$ , is a member of the group.<sup>12</sup> Below the antiferromagnetic transition,  $K$  is no longer a symmetry element, and the inversion operation  $I$  is replaced by the antiunitary operation of inversion followed by time reversal,  $KI$ . The magnetic structure is described by the magnetic space group  $R\bar{3}'c'$ . The irreducible representations of the magnetic group are obtained by considering the representations of the subgroup which contains only unitary operators.<sup>13</sup> The group  $R\bar{3}'c'$  has the symmetry elements  $\{E|0\}$ ,  $2\{C_3|0\}$ ,  $3\{C_2'|\tau\}$ ,  $\{KI|0\}$ ,  $2\{KS_6|0\}$ , and  $3\{K\sigma_d|\tau\}$ . The unitary subgroup is  $R32$ . This group is also the group of the  $\mathbf{k}$  vector at the center of the Brillouin zone, and the representations of both groups will be designated by the same symbols. Analysis of the magnetic group shows that, with the addition of the antiunitary operator  $\{KI|0\}$ , the properties of the representations of  $R32$  in the magnetic group  $R\bar{3}'c'$  are the same as the time-reversal properties of the representations of  $R32$ .<sup>13</sup> In particular, no new degeneracy is introduced for the single-valued representations.

The character table for the site symmetry  $C_3$ , the  $\mathbf{k}=0$  point of the paramagnetic group  $R\bar{3}c$ , and the group  $R32$  are shown in Tables II and III.<sup>14</sup> The rep-

TABLE II. Character table for the point group  $C_3=3$ . The pairs of representations ( $C_1, C_2$ ) and ( $S_1, S_2$ ) are Kramers degenerate.  $\omega = \exp(i\pi/3)$ .

		$E$	$C_3$	$C_3^{-1}$		
$A$	$\Gamma_1$	1	1	1		
$C_1$	$\Gamma_2$	1	$\omega^2$	$-\omega$		
$C_2$	$\Gamma_3$	1	$-\omega$	$\omega^2$		
$S_1$	$\Gamma_4$	1	$\omega$	$-\omega$	$-\omega^2$	$\omega^2$
$S_2$	$\Gamma_5$	1	$-\omega$	$\omega$	$-\omega^2$	$\omega^2$
$S_3$	$\Gamma_6$	1	$-\omega^2$	$\omega^2$	$\omega$	$-\omega$

<sup>12</sup> B. A. Tavger and V. M. Zaitzev, *Zh. Eksperim. i Teor. Fiz.* **30**, 564 (1956) [English transl.: *Soviet Phys.—JETP* **3**, 430 (1956)]; N. V. Belov, N. N. Neronova, and T. S. Smirnova, *Trudy Inst. Krist.* **11**, 33 (1955) [English transl.: *Soviet Phys.—Cryst.* **2**, 311 (1957)]. Magnetic symmetry has been discussed by W. Opechowski and R. Guccione [*Magnetism*, edited by G. T. Rado and H. Suhl (Academic Press Inc., New York, 1965), Vol. IIA, p. 105] and by Y. Le Corre [*J. Phys. Radium* **19**, 750 (1958)].

<sup>13</sup> J. O. Dimmock and R. G. Wheeler [*Phys. Chem. Solids* **23**, 729 (1962)] and J. O. Dimmock [*J. Math. Phys.* **4**, 1307 (1963)] have discussed the irreducible representations of the nonunitary groups.

<sup>14</sup> G. F. Koster, J. O. Dimmock, R. G. Wheeler, and H. Statz, *Properties of the Thirty-Two Point Groups* (McGraw-Hill Book Company, Inc., New York, 1962).

TABLE III. Character table for the point  $\mathbf{k}=0$  of the groups  $R32$  and  $R\bar{3}C$ .<sup>a</sup>

$R32$	$R\bar{3}C$	$\begin{Bmatrix} E \\ E \end{Bmatrix}   0$	$\begin{Bmatrix} 2\{C_3 \\ 2\{C_3 \end{Bmatrix}   0$	$\begin{Bmatrix} 3\{C_2' \\ 3\{C_2' \end{Bmatrix}   \tau$	$\{I   0\}$	$2\{S_6   0\}$	$3\{\sigma_d   \tau\}$
$\Gamma_1$	$\Gamma_1^+$	1	1	1	1	1	1
	$\Gamma_1^-$	1	1	1	-1	-1	-1
$\Gamma_2$	$\Gamma_2^+$	1	1	-1	1	1	-1
	$\Gamma_2^-$	1	1	-1	-1	-1	1
$\Gamma_3$	$\Gamma_3^+$	2	-1	0	2	-1	0
	$\Gamma_3^-$	2	-1	0	-2	1	0

<sup>a</sup>  $\tau = \frac{1}{2}(t_1 + t_2 + t_3)$ .

representations are identified both by Mulliken and Bethe notation. For clarity we shall use the Mulliken notation when discussing the site symmetry and reserve the  $\Gamma$  nomenclature for the  $\mathbf{k}=0$  excitons. From Table III we find that the representations  $\Gamma_i^\pm (i=1, 2, 3)$  of the group  $R\bar{3}C$  reduce to  $\Gamma_i$  in the group  $R32$ . In the antiferromagnetic phase the excitons no longer have a definite parity. Although the exchange interaction has important effects on the splitting of the exciton levels, its effect on the coupling of the exciton levels to the optical radiation field is small. In considering optical absorption processes we shall thus describe the excitons by their paramagnetic space group representations, keeping in mind, however, the effects of the reduction in symmetry in going to the antiferromagnetic phase.

The selection rules for radiative transitions are obtained from the transformation properties of the multipole moments given in Table IV. The change in the crystal quantum number  $\Delta\mu$  is given in the last column.

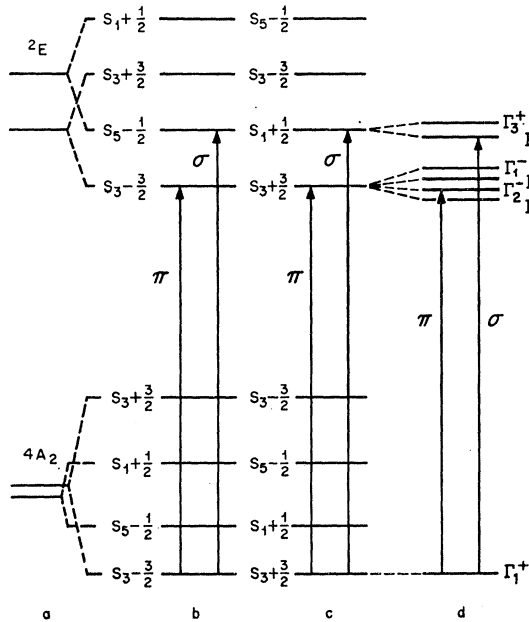


FIG. 2. Derivation of the exciton spectrum based on the molecular-field model. The crystal-field levels (a) are split by the molecular field as shown in (b, c) for the two sublattices. The transitions combine to form the excitons (d).

Both  ${}^2E$  and  ${}^4A_2$  transform as  $D_{3/2}$  in  $O_h$ , and split under the combined action of the trigonal field and spin-orbit interaction into two pairs of degenerate levels transforming as the representations  $2S_3$  and  $S_1, S_5$ . The molecular field acting on the spatially quantized spins on the two sublattices yields the splitting pattern shown in Figs. 2(b) and 2(c).

Electric dipole transitions are not allowed between  ${}^4A_2$  and  ${}^2E$ . In symmetry  $C_3$ , the transition operators originating from the lowest-energy single-ion levels transform as  $S_3 \times S_3^* = A, S_1 \times S_3^* = C_2$ , and  $S_5 \times S_3^* = C_1$ . The electric dipole transitions shown in Figs. 2(b) and 2(c) are obtained when the additional selection rule for the crystal quantum number is applied.

From Eq. (1) the single-ion  $A$  transition operator results in four  $\mathbf{k}=0$  excitons having symmetry  $\Gamma_1^\pm$  and  $\Gamma_2^\pm$ . The  $C_1$  and  $C_2$  transition operators combine to yield  $\Gamma_3^+$  and  $\Gamma_3^-$  excitons. The group-theoretical arguments used here are somewhat different from those used in Ref. 1. There the exciton levels were incorrectly stated to be doubly degenerate. The interpretation of the experimental results is unchanged if we identify the  $\Gamma_1, \Gamma_2, \Gamma_3$  excitons of Ref. 1 with the  $\Gamma_1^-, \Gamma_2^-, \Gamma_3^-$  excitons of this paper. Electric dipole transitions are allowed to  $\Gamma_3^-$  for  $\sigma$ -polarized radiation, and to  $\Gamma_2^-$  for  $\pi$  polarization. From consideration of the magnetic space group, much weaker electric dipole absorption is also expected to the states labeled  $\Gamma_2^+$  and  $\Gamma_3^+$  in Fig. 2(d). The energies of the excitons originating from the same single-ion transition are sep-

TABLE IV. Transformation properties of the multipole moments.

	Polarization	Representation			$\Delta\mu$
		3	$R\bar{3}C$	$R32$	
<b>Electric dipole</b>					
$-i(x+iy)$	$\sigma, a$	$C_1$	$\Gamma_3^-$	$\Gamma_3$	1
$x-iy$	$\sigma, a$	$C_2$	$\Gamma_3^-$	$\Gamma_3$	-1
$z$	$\pi$	$A$	$\Gamma_2^-$	$\Gamma_2$	0
<b>Magnetic dipole</b>					
$-(L_x+iL_y)$	$\pi, a$	$C_1$	$\Gamma_3^+$	$\Gamma_3$	1
$L_x-iL_y$	$\pi, a$	$C_2$	$\Gamma_3^+$	$\Gamma_3$	-1
$L_z$	$\sigma$	$A$	$\Gamma_2^+$	$\Gamma_2$	0

arated by the Davydov splittings, which result from the exchange of excitation between translationally inequivalent ions. As shown in Sec. III, the splittings are expected to be at most several wave numbers. Thus only two strong lines are predicted by the above theory, while four lines are observed. This difficulty was previously encountered by Wickersheim<sup>8</sup> with the single-ion molecular-field approximation. The presence of the two additional absorption lines does not appear to be due to the mixing of the  $S_z = \pm \frac{3}{2}$  ground-state functions. The wave function  $0.96 | \frac{3}{2} \rangle + 0.2 | -\frac{3}{2} \rangle$  reduces the sublattice magnetic moment to the experimentally observed<sup>11</sup>  $2.76\mu_B$  from its spin-only value of  $3\mu_B$ . The ratio of the upper to lower  $\sigma$ -polarized absorption cross sections is 0.042, an order of magnitude smaller than the experimental value of 0.56 obtained from Table I. A similar result obtains when mixing of the  $S_z = \frac{1}{2}$  with  $S_z = \frac{3}{2}$  is considered. Pratt and Bailey<sup>15</sup> were able to explain the temperature dependence of the susceptibility using the Oguchi pair method, but by applying this theory to the  ${}^2E$  state they also obtained only two transitions with an appreciable dipole moment to these levels from the lowest level of the ground state.

The energy separations between the upper and lower  $\sigma$  and  $\pi$  polarized lines are 184.4 and 140  $\text{cm}^{-1}$ , respectively. This effectively rules out the possibility that the upper lines may be magnon side bands of the lower-energy absorption lines since, as will be shown from the fluorescence data of Sec. IV, the sidebands would be expected to be about 250  $\text{cm}^{-1}$  above the sharp lines.

Electric dipole transitions to the upper  ${}^2E$  levels would occur if the selection rules of the crystal quantum number,  $\Delta\mu = \pm 1$  for  $\sigma$  transitions and zero for  $\pi$  transitions, are relaxed. Since the selection rules are quite valid for ruby with magnetic field parallel to the threefold axis,<sup>16</sup> there appears to be no *a priori* reason for discarding them for  $\text{Cr}_2\text{O}_3$  in the molecular-field approximation.

Transitions to the upper levels may be obtained by mixing the two  $S_3$ -symmetry excited single-ion states and the  $S_1$  and  $S_6$  states. We shall generalize the molecular-field approximation to take into account the effects of a non- $S$ -orbital state on the exchange. We apply the effective Hamiltonian method used by Tanabe and Kamimura<sup>17</sup> for the  ${}^2E$  state of ruby, and shall follow their phase conventions and definitions. The effective Hamiltonian contains only terms which have matrix elements within the excited state. For the  ${}^2E$  state, the spin operator can appear linearly and the allowed orbital functions transform as the irreducible representation  $A_1$ ,  $A_2$ , and  $E$  of the octahedral group. In the trigonal site symmetry, the Hermitian functions

<sup>15</sup> G. W. Pratt, Jr., and P. T. Bailey, Phys. Rev. **131**, 1923 (1963).

<sup>16</sup> S. Sugano and I. Tsujikawa, J. Phys. Soc. Japan **13**, 899 (1958).

<sup>17</sup> Y. Tanabe and H. Kamimura, J. Phys. Soc. Japan **13**, 394 (1958).

having real matrix elements are  $V(A_1)$  and the two components of the  $E$  representation,  $V(u_+)$  and  $V(u_-)$ . The function transforming as  $A_2$  is a pure imaginary operator and is denoted by  $T(A_2)$ . Since the ions near the excited ion are in the  ${}^4A_2$  state, the exchange field enters linearly in lowest order.<sup>7</sup> These factors are combined to yield a  $\mathcal{H}_{\text{eff}}$  transforming as the symmetric representation of the point group  $C_3$ , and which is invariant under time reversal. In its most general form, the  $\mathcal{H}_{\text{eff}}$  which operates on the wave functions  $|u_+ + \frac{1}{2}\rangle$ ,  $|u_+ - \frac{1}{2}\rangle$ ,  $|u_- + \frac{1}{2}\rangle$ , and  $|u_- - \frac{1}{2}\rangle$  is

$$\begin{aligned} \mathcal{H}_{\text{eff}} = & \lambda S_z T(A_2) + g_{||} \beta H_z S_z + g_{||}' \beta H_z T(A_2) \\ & + g_{||}^E \beta H_z [V(u_+) S_- + V(u_-) S_+] \\ & + g_{\perp}^E \beta [H_+ V(u_+) S_+ - H_- V(u_-) S_-], \quad (2) \end{aligned}$$

where  $\lambda$ ,  $g_{||} H_z$ ,  $g_{||}' H_z$ ,  $g_{||}^E H_z$ , and  $g_{\perp}^E H_+$  are empirical parameters determined by experiment. The first term is the zero-field splitting of the  ${}^2E$  state and is caused by the combined action of the trigonal field and the spin-orbit interaction. The second term is the molecular-field contribution, the third includes spin-orbit and crystal-field contributions, and the possible effects of exchange on the orbital function. The Zeeman spectrum of  $\text{Al}_2\text{O}_3:\text{Cr}^{3+}$  is accurately described by the first three terms. The remaining terms express the effect of the exchange field on the combined spin and orbital functions. Using the  $u_+$ ,  $u_-$  basis functions of  $E$ , one has, on absorbing all numerical factors in the empirical parameters, the two-dimensional matrices

$$\begin{aligned} T(A_2) &= \begin{pmatrix} 1 & 0 \\ 0 & -1 \end{pmatrix}, \\ V(u_+) &= \begin{pmatrix} 0 & 0 \\ -1 & 0 \end{pmatrix}, \\ V(u_-) &= \begin{pmatrix} 0 & 1 \\ 0 & 0 \end{pmatrix}. \quad (3) \end{aligned}$$

The eigenvalues and eigenfunctions of  $\mathcal{H}_{\text{eff}}$  are

$$E_1 = -\frac{1}{2}\lambda + (\frac{1}{2}g_{||} - g_{||}')\beta H_z - (1/\sqrt{2})g_{\perp}^E\beta |H_+ | \cot\theta, \quad (4a)$$

$$E_4 = -\frac{1}{2}\lambda - (\frac{1}{2}g_{||} - g_{||}')\beta H_z + (1/\sqrt{2})g_{\perp}^E\beta |H_+ | \cot\theta, \quad (4b)$$

with

$$\Psi_1 = |u_+ - \frac{1}{2}\rangle \cos\theta - |u_- + \frac{1}{2}\rangle e^{i\eta} \sin\theta, \quad (5a)$$

$$\Psi_4 = |u_+ - \frac{1}{2}\rangle \sin\theta + |u_- + \frac{1}{2}\rangle e^{-i\eta} \cos\theta, \quad (5b)$$

where  $e^{i\eta} = H_+ / |H_+ |$ , and

$$E_2 = \frac{1}{2}\lambda + (\frac{1}{2}g_{||} + g_{||}')\beta H_z - (1/\sqrt{2})g_{||}^E\beta H_z \cot\phi, \quad (6a)$$

$$E_3 = \frac{1}{2}\lambda - (\frac{1}{2}g_{||} + g_{||}')\beta H_z + (1/\sqrt{2})g_{||}^E\beta H_z \cot\phi, \quad (6b)$$

$$\Psi_2 = |u_- - \frac{1}{2}\rangle \cos\phi + |u_+ + \frac{1}{2}\rangle \sin\phi, \quad (7a)$$

$$\Psi_3 = |u_- - \frac{1}{2}\rangle \sin\phi - |u_+ + \frac{1}{2}\rangle \cos\phi, \quad (7b)$$

where the phases  $\theta$ ,  $\phi$  are

$$\tan 2\theta = \sqrt{2}g_{\perp}^E |H_+| / (g_{\parallel} - 2g_{\parallel}')H_z, \quad (8)$$

$$\tan 2\phi = \sqrt{2}g_{\parallel}^E / (g_{\parallel} + 2g_{\parallel}'). \quad (9)$$

Considering only the first three terms of  $\mathcal{H}_{\text{eff}}$ , the  ${}^4A_2(S_z = -\frac{3}{2})$  state has a  $\sigma$ -polarized transition to  ${}^2E(u_+ - \frac{1}{2})$  and a  $\pi$ -polarized transition to  ${}^2E(u_- - \frac{1}{2})$ . With the complete  $\mathcal{H}_{\text{eff}}$  the states are mixed and transitions are now allowed to all four states with absorption strengths given by

$$\sigma_1 = \sigma \cos^2\theta \quad \pi_1 = 0, \quad (10a)$$

$$\sigma_4 = \sigma \sin^2\theta \quad \pi_4 = 0, \quad (10b)$$

$$\pi_2 = \pi \cos^2\phi \quad \sigma_2 = 0, \quad (10c)$$

$$\pi_3 = \pi \sin^2\phi \quad \sigma_3 = 0, \quad (10d)$$

where  $\sigma$  and  $\pi$  are the dipole strengths from  $S_z = -\frac{3}{2}$  to the  ${}^2E$  levels in the absence of exchange.

The exciton spectrum corresponding to these single-ion transitions is shown in Fig. 3 for the case the last terms of  $\mathcal{H}_{\text{eff}}$  are large compared to the first three terms and  $g_{\perp}^E |H_+| > g_{\parallel}^E H_z$ . There are now two  $\sigma$ - and two  $\pi$ -polarized transitions, and as in the molecular-field approximation the twofold degenerate  $\Gamma_3^-$  exciton is split by a magnetic field, but the nondegenerate  $\Gamma_1^-$  and  $\Gamma_2^-$  excitons are not.

### III. ABSORPTION

The absorption data shown in Table I were obtained using a 1-m Czerny-Turner spectrometer and a S-20 response photomultiplier. Samples, in the form of oriented plates, were prepared from boules grown by R. A. Lefever. The absorption lines of these crystals were found to be about  $5 \text{ cm}^{-1}$  higher in energy than the values given by Wickersheim.<sup>3</sup> Some additional measurements were made on thin  $c$ -axis platelets which were grown by H. J. Guggenheim using a flux technique. The absorptions of the upper and lower  $\sigma$ -polarized lines for these crystals were found to be, respectively,  $1.8$  and  $1.0 \text{ cm}^{-1}$  higher in energy than the values shown in Table I, and the linewidths were smaller. The variation in peak absorption energy appears to depend on the degree of long-range crystal perfection. The deviation from perfect polarization results mainly from a slight variation of the  $c$ -axis direction throughout the crystal such as is often found in Verneuil grown crystals. X-ray measurements also indicated the presence of several small crystallites. The axial spectrum of the flux-grown crystal, however, was very well polarized.

The  $\text{Cr}_2\text{O}_3$  cross sections may be compared to the values obtained by Nelson and Sturge<sup>18</sup> for  $\text{Al}_2\text{O}_3:\text{Cr}^{3+}$ . Taking into account the theory of Sec. II and the depolarization, it is the total  $\sigma$ - and  $\pi$ -polarized cross sections of Table I,  $1.9 \times 10^{-19} \text{ cm}$  and  $0.85 \times 10^{-19} \text{ cm}$ , respectively, which are to be compared to one-half their

<sup>18</sup> D. F. Nelson and M. D. Sturge, Phys. Rev. **137**, A1117 (1965).

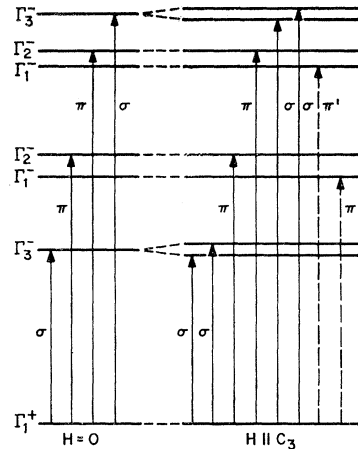


FIG. 3. Modification of the exciton spectrum introduced by the exchange interaction discussed in the text. Only the electric dipole active excitons are shown. The order of the levels depends on the values of the empirical parameters. Transitions to the  $\Gamma_1^-$  excitons, labeled  $\pi'$ , become allowed in a magnetic field.

ruby values for the  $S_z = \pm \frac{3}{2}$  state, namely  $1.7 \times 10^{-19}$  and  $0.38 \times 10^{-19} \text{ cm}$ . The near equality of the cross sections, although interesting, is not significant since both the position and the strength of the  ${}^4T_2$  bands from which the  ${}^2E$  lines borrow their intensity through spin-orbit coupling are not the same for the two crystals.

Using the theory of Sugano and Tanabe,<sup>19</sup> the  ${}^2E$  cross sections can be calculated from McClure's absorption data for the  ${}^4T_2$  band.<sup>2</sup> With  $\zeta' = 153 \text{ cm}^{-1}$ ,<sup>20</sup> the cross sections are found to be  $10.2 \times 10^{-19} \text{ cm}$  for  $\sigma$  and  $6.25 \times 10^{-19} \text{ cm}$  for  $\pi$  polarization. The poor agreement can be only partially attributed to the uncertainty of the  ${}^4T_2$  absorption data, and to a lesser extent to the  ${}^2E$  absorption results. The major cause for the discrepancy probably results from not including the phonon-assisted contribution to the  ${}^2E$  cross section. Since the  ${}^2E$  levels are relatively closer to the  ${}^4T_2$  band than is the case for ruby, the transition in  $\text{Cr}_2\text{O}_3$  is expected to be relatively more sensitive to the crystal field.<sup>21</sup>

In the above, we have implicitly assumed that the absorption cross sections are given by the single-ion values. The empirical parameters of  $\mathcal{H}_{\text{eff}}$  can be found if we assume the energy levels are given by the single-ion values, Eqs. (4) and (6). The latter implies equal band shifts<sup>5</sup> of all the excitons. In view of the assumptions made, the values shown in Table V, obtained from the experimental data given in Table I, should be regarded with some caution. It does indicate, however, that the last terms of  $\mathcal{H}_{\text{eff}}$  clearly predominate over the molecular-field term.<sup>22</sup>

<sup>19</sup> S. Sugano and Y. Tanabe, J. Phys. Soc. Japan **13**, 880 (1958).

<sup>20</sup> S. Sugano and M. Peter, Phys. Rev. **122**, 381 (1961).

<sup>21</sup> M. D. Sturge (private communication).

<sup>22</sup> From the second and fourth lines of Table V, we obtain  $g_{\parallel}' = -0.24 (g_{\parallel}/2)$ . This is consistent with the calculation of R. M. Macfarlane [Bull. Am. Phys. Soc. **11**, 243 (1966)] if we interpret these quantities as true  $g$  values, and accept reasonable values for the trigonal field parameters [M. D. Sturge (private communication)].

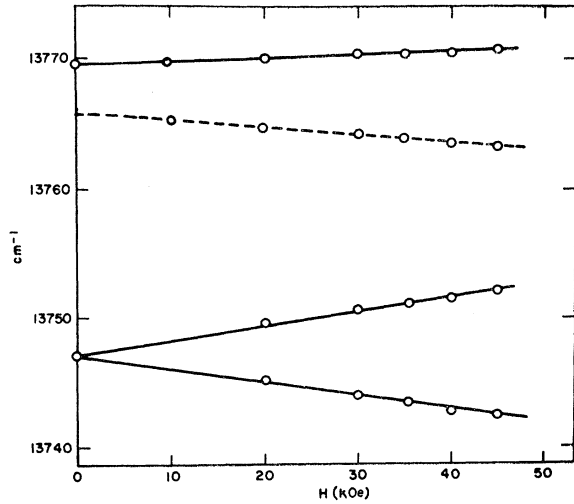


FIG. 4. Field dependence of the low-energy absorption lines at 13 747.0  $\text{cm}^{-1}$  ( $\sigma$ ) and 13 769.5  $\text{cm}^{-1}$  ( $\pi$ ) for  $H$  parallel to the  $c$  axis. The field-dependent satellite absorption near 13 765  $\text{cm}^{-1}$  is shown by the dashed line.

As shown in Table IV, electric and magnetic dipole transitions to the  $\Gamma_1$  exciton (magnetic group) are not allowed. They may occur if the symmetry is lowered. For example, a magnetic field applied parallel to the  $c$  axis removes the symmetry operations  $\{KI|0\}$ ,  $\{KS_6|0\}$ ,  $\{C_2'|\pi\}$  and introduces a unique sense of rotation about the  $c$  axis. The symmetry of the magnetic space group and its unitary subgroup is reduced to  $R3$ . The character table for the  $\mathbf{k}=0$  point is found from Table II. The  $\Gamma_1$  and  $\Gamma_2$  excitons reduce to the exciton  $\Gamma_1$  of  $R3$ , and  $\pi$ -polarized transitions to both are allowed. In the paramagnetic space group the magnetic moment transforms as  $\Gamma_2^+$ , and transitions to  $\Gamma_1^-$  become allowed. In this approximation, electric dipole transitions to  $\Gamma_1^+$  and  $\Gamma_2^+$  are forbidden.

We consider now the combined effects of the interaction leading to the Davydov splitting and the magnetic field. The four-exciton wave functions resulting from the  $A$  single-ion transitions, in terms of the one-

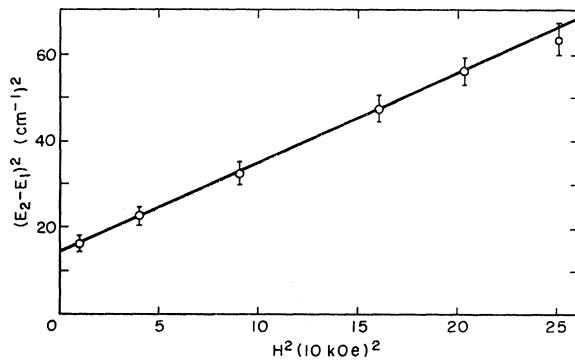


FIG. 5. Field dependence of the energy separation between the  $\Gamma_1^-$  and  $\Gamma_2^-$  excitons.

site exciton wave functions are

$$\begin{aligned}\phi_1 &= \phi(\Gamma_1^-) = \frac{1}{2}[\phi_a^\pi + \phi_b^\pi - \phi_c^\pi - \phi_d^\pi], \\ \phi_2 &= \phi(\Gamma_2^-) = \frac{1}{2}[\phi_a^\pi - \phi_b^\pi + \phi_c^\pi - \phi_d^\pi], \\ \phi_3 &= \phi(\Gamma_1^+) = \frac{1}{2}[\phi_a^\pi + \phi_b^\pi + \phi_c^\pi + \phi_d^\pi], \\ \phi_4 &= \phi(\Gamma_2^+) = \frac{1}{2}[\phi_a^\pi - \phi_b^\pi - \phi_c^\pi + \phi_d^\pi].\end{aligned}\quad (11)$$

Here  $\phi_a^\pi$ ,  $\phi_b^\pi$ ,  $\phi_c^\pi$ , and  $\phi_d^\pi$  are linear combinations of antisymmetrized products of single-ion wave functions with the excitation distributed, respectively, over the  $a$ ,  $b$ ,  $c$ , and  $d$  sites of Fig. 1. The wave functions have the symmetry of the paramagnetic space group. Since the dipole moments parallel to the  $c$  axis on sites  $a$  and  $c$  are opposed to the direction of the dipole moments of the sites  $b$  and  $d$ , only  $\phi_2$  has a dipole moment with the ground state.

The Hamiltonian may be separated in two parts,

$$\mathcal{H} = \mathcal{H}' + \mathcal{H}'', \quad (12)$$

where  $\mathcal{H}'$  and  $\mathcal{H}''$  have, respectively, off-diagonal and diagonal matrix elements with the one-site excitons. The term  $\mathcal{H}'$  gives the Davydov splittings. From symmetry, we obtain  $\mathcal{H}'_{ab} = \mathcal{H}'_{cd}$ ,  $\mathcal{H}'_{ac} = \mathcal{H}'_{bd}$ , and  $\mathcal{H}'_{bc} =$

TABLE V. Experimentally determined values of the parameters appearing in  $\mathcal{H}'_{\text{eff}}$  [Eq. (2)].

$g_1^2 \beta  H_+ /\sqrt{2}$	88.2 $\text{cm}^{-1}$
$(\frac{1}{2}g_{11} - g_{11}')\beta H_z$	25.8 $\text{cm}^{-1}$
$g_{11}^2 \beta H_z/\sqrt{2}$	68.5 $\text{cm}^{-1}$
$(\frac{1}{2}g_{11} + g_{11}')\beta H_z$	15.4 $\text{cm}^{-1}$

$\mathcal{H}'_{ad}$ .  $\mathcal{H}'$  has only diagonal matrix elements with the wave functions of Eq. (11).

$$\mathcal{H}'_{ii} = \frac{1}{2} \begin{pmatrix} + & - & - & - & - & + \\ - & + & - & - & + & - \\ \mathcal{H}'_{ab} & \mathcal{H}'_{ac} & \mathcal{H}'_{ad} & \mathcal{H}'_{bc} & \mathcal{H}'_{bd} & \mathcal{H}'_{cd} \\ + & + & + & + & + & + \\ - & - & + & + & - & - \end{pmatrix}, \quad (13)$$

where  $i = 1, 2, 3, 4$ .

The magnetic field dependence of the excitons is contained in  $\mathcal{H}''$ . Its matrix elements are related by

$$\mathcal{H}''_{aa} = -\mathcal{H}''_{bb} = \mathcal{H}''_{cc} = -\mathcal{H}''_{dd}.$$

$\mathcal{H}''$  has off-diagonal matrix elements with excitons  $\Gamma_1^-$  and  $\Gamma_2^-$ . The eigenvalues of the Hamiltonian, Eq. (12), are

$$E = \frac{1}{2} \{ \mathcal{H}'_{11} + \mathcal{H}'_{22} \pm [ (\mathcal{H}'_{11} - \mathcal{H}'_{22})^2 + 4(\mathcal{H}'_{12})^2 ]^{1/2} \}. \quad (14)$$

A similar result obtains for the  $\Gamma_1^+$  and  $\Gamma_2^+$  excitons. The term in  $\mathcal{H}''$  is found not to have matrix elements with excitons of different parity. Matrix elements of Eq. (11) between the exciton states which are separated by the exchange interaction are of second order, and have not been included.

Using the wave functions, Eq. (11), the electric dipole moments parallel to the  $c$  axis to the exciton levels are

$$\langle \phi_i | Z | \phi_0 \rangle = \frac{1}{2} \begin{pmatrix} + & + & - & - \\ + & - & + & - \\ Z_{a0} & Z_{b0} & Z_{c0} & Z_{d0} \\ + & + & + & + \\ + & - & - & + \end{pmatrix}.$$

The dipole moments of sites  $b$  and  $d$  are opposed to the direction of the moments on sites  $a$  and  $c$ . A positive dipole moment is taken to be parallel to the defined positive direction of the crystal trigonal axis. With the wave functions Eq. (11) we have  $Z_{a0} = -Z_{b0} = Z_{c0} = -Z_{d0}$  and a dipole moment exists only to the  $\Gamma_2^-$  exciton.

The wave functions Eq. (11) transform correctly under the operations of the antiferromagnetic group. Using these symmetry operations we have  $Z_{a0} = -Z_{b0}$  and  $Z_{c0} = -Z_{d0}$ . Thus, in addition to the  $\Gamma_2^-$  absorption there is a possible absorption to the state labeled  $\Gamma_2^+$  which results from the incomplete cancellation of the site dipole moments. This is of course consistent with the reduction in symmetry ( $\Gamma_2^\pm \rightarrow \Gamma_2$ ) given in Table III. Transitions to  $\Gamma_1^\pm$  remain forbidden. The difference between  $Z_{a0}$  and  $Z_{c0}$  results from the exchange interaction; for  $\text{Cr}_2\text{O}_3$  this is expected to be negligible. This is the justification for using the paramagnetic space group representations.

Figure 4 shows the field dependence of the energy levels of the lower excitons. The field was produced by a superconducting solenoid. We identify the lower exciton as  $\Gamma_3^-$  by its linear splitting. The  $\Gamma_2^-$  exciton is seen to shift to higher energy and an additional  $\pi$ -polarized absorption line appears on the low-energy side of this absorption. The latter is the behavior expected of the  $\Gamma_1^-$  exciton. The field dependence of the energy separation between the  $\Gamma_1^-$  and  $\Gamma_2^-$  excitons is shown in greater detail in Fig. 5. The square of the energy separation is plotted as a function of the square of the applied field. The line is a plot of the equation

$$(E_2 - E_1)^2 = 14.1 + 2.06H^2 \text{ (cm}^{-1}\text{)}^2, \quad (15)$$

where  $H$  is in units of 10 kOe. Comparing with Eq. (14) and taking note of the limits of experimental error, we find a Davydov splitting of  $\mathcal{H}_{22}' - \mathcal{H}_{11}' = 3.75 (\pm 0.25) \text{ cm}^{-1}$ . The square root of the slope yields

$$2\mathcal{H}_{12}''/H = 0.143 \text{ (cm}^{-1}\text{/kOe)}. \quad (16)$$

It is of interest to obtain a numerical estimate of the matrix elements of  $\mathcal{H}'$  and thus find the mechanism responsible for the splitting. The interactions which result in the exchange of excitation between ions is of central importance in theories of sensitized luminescence, and have been discussed by Dexter.<sup>23</sup> More re-

<sup>23</sup> D. L. Dexter, J. Chem. Phys. **21**, 836 (1953); Phys. Rev. **126**, 1962 (1962).

cently, Imbusch<sup>24</sup> has applied the theory to energy transfer processes in  $\text{Al}_2\text{O}_3:\text{Cr}^{3+}$ . We shall extend his work to the case of  $\text{Cr}_2\text{O}_3$ .

Consider first the splitting due to the exchange interaction  $J_{12}\mathbf{S}_1 \cdot \mathbf{S}_2$ . This term has no first-order matrix elements between the  ${}^2E$  and  ${}^4A_2$  levels. A matrix element is obtained only by including the spin-orbit interaction, coupling both the  ${}^4A_2$  and  ${}^2E$  to the  ${}^4T_2$  state. Using  $J_{12}\mathbf{S}_1 \cdot \mathbf{S}_2 = 250 \text{ cm}^{-1}$ ,  $\zeta' = 153 \text{ cm}^{-1}$ ,<sup>20</sup> and the  ${}^4T_2$  energy of  $16\,500 \text{ cm}^{-1}$  from Ref. 2, the matrix element

$$J_{12}\mathbf{S}_1 \cdot \mathbf{S}_2 \{ (\zeta')^2 / [E({}^4T_2) - E({}^2E)] [E({}^4T_2) - E({}^4A_2)] \}^2$$

is of the order of  $10^{-4}$ . As this is four orders of magnitude too small, we rule out the exchange interaction as the dominant mechanism.

We next consider the contributions obtained from the multipole moments of the electrostatic interaction. Between ions  $a$  and  $b$  we have

$$\begin{aligned} \mathcal{H}' = & -d_i^{(a)}d_j^{(b)}\nabla_i\nabla_j | R |^{-1} \\ & + \frac{1}{2}(d_i^{(a)}Q_{jk}^{(b)} + d_i^{(b)}Q_{jk}^{(a)})\nabla_i\nabla_j\nabla_k | R |^{-1} \\ & + \frac{1}{4}Q_{ij}^{(a)}Q_{kl}^{(b)}\nabla_i\nabla_j\nabla_k\nabla_l | R |^{-1} + \dots, \quad (17) \end{aligned}$$

where  $i, j, k, l$  refer to the Cartesian coordinates, and the summation convention is implied. The dipole moment of ion  $a$  is  $d_i^{(a)} = e \sum r_i^{(a)}$  and the quadrupole moment is  $Q_{ij}^{(a)} = e \sum (r_i^{(a)}r_j^{(a)} - \delta_{ij} |\mathbf{r}^{(a)}|^2/3)$ . The sum is over the electrons of the ion.

In a solid the interaction between well-separated ions is reduced by the dielectric shielding of the intervening medium. However, for the case of near-neighbor pairs, the situation may not be as simple. Thus for the order-of-magnitude calculation given below, we will *not* include the effects of shielding.

The first term gives the dipole-dipole interaction. The matrix element of  $\mathcal{H}'$  includes matrix elements of the dipole moment, the latter may be expressed in terms of the electric dipole oscillator strength

$$|\langle d \rangle|^2 = (3\hbar e^2/2m\omega)f_d.$$

The matrix element of the dipole-dipole term approximately is

$$V_d \approx 3\hbar e^2 f_d / 2m\omega R^3. \quad (18)$$

Substituting the measured electric dipole oscillator strength of the  $\Gamma_2^-$  level,  $f_d = 2.5 \times 10^{-8}$ , and the nearest-neighbor distance of  $2.65 \text{ \AA}$ ,<sup>2</sup> we obtain  $V_d \approx 10^{-3} \text{ cm}^{-1}$ . This is again too small.

The quadrupole-quadrupole interaction is given by the third term in Eq. (17). Imbusch has shown that, for  $\text{Cr}^{3+}$  in  $\text{Al}_2\text{O}_3$ , a quadrupole matrix element exists between  ${}^4A_2$  and  ${}^2E$  if the spin-orbit interaction of the  ${}^4A_2$  with the  ${}^2T_2$  level is taken into account. The quad-

<sup>24</sup> G. F. Imbusch, Phys. Rev. **153**, 326 (1967).

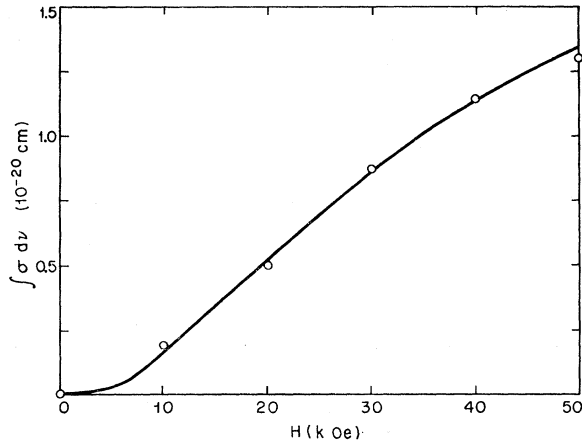


FIG. 6. Integrated absorption cross section of the satellite line as a function of the field. The curve is calculated from Eq. (20) using the parameters discussed in the text.

rupole oscillator strength

$$f_q = (m\omega/3\hbar) (\pi/\lambda)^2 \sum_{i \neq j} |\langle Q_{ij} \rangle|^2$$

for  $\text{Cr}^{3+}$  in  $\text{Al}_2\text{O}_3$  is calculated by Imbusch to have the value  $1.5 \times 10^{-11}$ . The matrix element of the quadrupole-quadrupole interaction is approximately

$$V_q \approx 3\hbar\lambda^2 f_q / 4\pi^2 m\omega R^5. \quad (19)$$

With the above value of  $f_q$ ,  $V_q$  is found to be  $0.25 \text{ cm}^{-1}$  for the nearest neighbors. This is somewhat smaller than the estimate given in Ref. 1. However, there is an additional numerical factor in the numerator of  $V_q$  which results from the derivatives of  $|R|^{-1}$ . This important factor depends on the relative values of the quadrupole matrix elements. It is estimated to increase the splitting approximately tenfold. The matrix element of the dipole-quadrupole interaction [the second term in Eq. (17)] has a value intermediate between  $V_a$  and  $V_q$ . The higher-order multipole interactions may be shown to be negligibly small. As has been found<sup>24</sup> for  $\text{Al}_2\text{O}_3:\text{Cr}^{3+}$ , the quadrupole-quadrupole coupling appears to be the predominant energy-transfer mechanism.

Neighbors more distant than the first also make important contributions to the splitting. Referring to ion  $a$  in Fig. 1, the nearest neighbor is of the type  $a-b$ . There are three second neighbors of the type  $a-d$  where  $a$  and  $d$  are in different unit cells, and three third neighbors  $a-b$  with  $b$  in yet another cell from the second-neighbor ion  $d$ . The separation between neighbors increases only slowly from the first to the fifth. An accurate numerical evaluation of the Davydov splitting thus requires the inclusion of a large number of terms. In addition the angular dependence of the quadrupole interaction should be taken into account. Such a calculation is beyond the scope of the present paper.

Another test of the theory is obtained from the field dependence of the integrated absorption cross section.

For the  $\Gamma_1^-$  exciton we have

$$\int \sigma(\Gamma_1^-) d\nu = \int \sigma_0(\Gamma_2^-) d\nu \frac{\{1 - [1 + (\epsilon H)^2]^{1/2}\}^2}{\{1 - [1 + (\epsilon H)^2]^{1/2}\}^2 + (\epsilon H)^2}, \quad (20)$$

where  $\sigma_0(\Gamma_2^-)$  is the  $\Gamma_2^-$  zero-field cross section, and

$$\epsilon^{-1} = (2\mathcal{J}C_{12}'')^{-1} (\mathcal{J}C_{22}' - \mathcal{J}C_{11}') H, \quad (21)$$

evaluated from the splitting data is 26.2 kOe. As shown in Fig. 6, a reasonably good fit is obtained by taking  $\int \sigma_0(\Gamma_2^-) d\nu = 5 \times 10^{-20}$  from the zero-field measurement. At 50 kOe about 25% of the zero-field  $\Gamma_2^-$  absorption has been transferred to the satellite.

The value of  $2\mathcal{J}C_{12}''$  enables us to calculate the field dependence of the two sublattices. Using Eqs. (11), (12), and (16), the difference in energy is

$$\mathcal{J}C_{aa}'' - \mathcal{J}C_{bb}'' = g_{\text{eff}} \beta H = 2\mathcal{J}C_{12}''. \quad (22)$$

Substituting from Eq. (16) gives  $g_{\text{eff}} = 3.06$ .

Figure 7 shows the field dependence of the upper excitons. The  $\Gamma_3^-$  exciton is split by the field; however, no satellite is found near the  $\Gamma_2^-$  exciton. A careful comparison of the  $\Gamma_2^-$  line shape, with and without field, indicated no change in the absorption strength or linewidth. With a 50-kOe field, the center of gravity shifts by less than  $0.5 \text{ cm}^{-1}$  from the zero-field value.

These observations are in qualitative agreement with the theory. Assuming the Davydov splittings are about the same for the upper and lower  $\pi$ -polarized lines, the magnitude of  $\mathcal{J}C_{12}''$  determines the coupling between the  $\Gamma_1^-$  and  $\Gamma_2^-$  excitons. Using Eqs. (7a) and (7b), the energy shifts of the site- $a$  exciton will be larger for the lower than the upper  $\pi$  excitons if  $\phi < \frac{1}{4}\pi$ . Consequently the coupling  $\mathcal{J}C_{12}''$  will be larger for the lower excitons. From Eq. (9) and Table V we obtain  $\phi = 38.7^\circ$ .

In another experiment, an electric field was applied

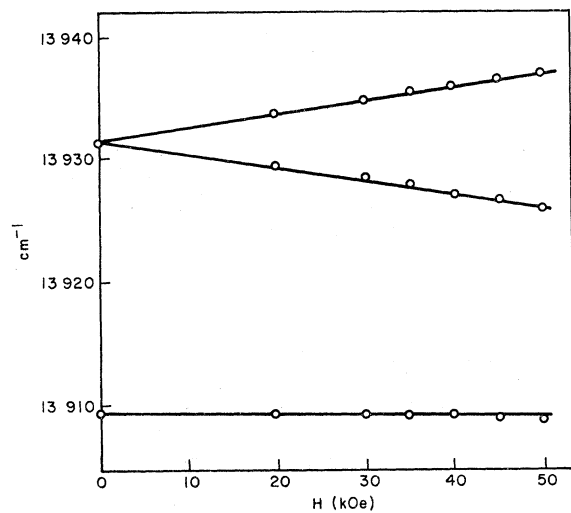


FIG. 7. Field dependence of the higher-energy absorption lines.

parallel to the  $c$  axis. This lowers the symmetry by destroying the center of inversion and the twofold axis. The glide plane remains, however, and the magnetic symmetry is reduced to  $R3c'$ . The unitary subgroup is  $R3$ . In first-order perturbation theory,  $\pi$ -polarized transitions become allowed to the  $\Gamma_1$  exciton, and the  $\Gamma_1$  and  $\Gamma_2$  energy levels will have a quadratic field dependence. The  $\Gamma_3$  exciton splits linearly with the applied field.

Aluminum strip electrodes were evaporated on the opposite faces of samples which were typically  $115 \mu$  thick. The light transmitted between the electrodes was measured at increasing field strengths, up to the field resulting in electrical breakdown and the destruction of the crystal. With a field of  $100 \text{ kV/cm}$ , the upper limit on any additional integrated absorption cross section was estimated to be less than  $0.05 \times 10^{-20} \text{ cm}$ , and any shift or broadening of the absorption lines was less than the experimental limit of  $0.2 \text{ cm}^{-1}$ .

A linear electric field effect has been observed in  $\text{Al}_2\text{O}_3:\text{Cr}^{3+}$ .<sup>25</sup> A field of  $100 \text{ kV/cm}$  is found to produce a splitting of  $0.53 \text{ cm}^{-1}$ . A linear splitting occurs because the net shifts of the levels of ions which are located on sites related by inversion are equal, but in opposite directions. The theory of this effect, based on an electronic mechanism, shows that the splitting is related to the value of the absorption cross section of the lines.<sup>26</sup>

In  $\text{Cr}_2\text{O}_3$ , the shift of the  $\Gamma_3$  exciton levels may be reduced to the shift of two chromium ions, one in the excited state, and the second, on the other sublattice, in the ground state. The two levels are shifted by equal amounts, but in opposing directions, giving a net splitting. Just as for the single ions in ruby, the  $\Gamma_3$  exciton splitting is equal to the difference between the shift of single-ion excited and ground-state levels. When the linear splitting is much smaller than the linewidth, it is manifest as a quadratic broadening of the line shape.<sup>27</sup> The upper limit of the lower-energy  $\Gamma_3$  exciton splitting of  $0.8 \text{ cm}^{-1}$  is obtained from the experimental limit of the broadening, and the Gaussian linewidth of  $2 \text{ cm}^{-1}$ .

#### IV. FLUORESCENCE

Figure 8 shows the near-infrared emission spectra of crystals grown by the Verneuil and flux techniques. In both cases the spectrum consists of a sharp line followed by a number of broad bands. The emission is obviously sample-dependent, and in both cases, the sharp line emission is shifted to lower photon energy

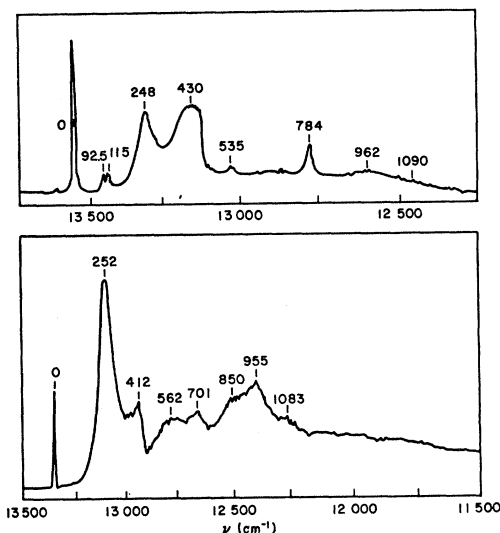


FIG. 8. Fluorescence from two  $\text{Cr}_2\text{O}_3$  crystals at  $4.2^\circ\text{K}$ . Top: Verneuil-grown crystal from R. A. Lefever. Bottom: Flux-grown crystal from H. J. Guggenheim.

as compared to the  ${}^2E$  absorption. No absorption is found to correspond to any of the emission wavelengths. These observations indicate that the fluorescence is not an intrinsic property of the crystal, but, as has also been observed in the antiferromagnetic transition-metal fluorides,<sup>28</sup> is the result of impurities. Neither is the emission solely characteristic of the impurities, rather it is thought that the impurities perturb the levels of nearby chromium ions via the electrostatic interaction, creating impurity-trap levels which lie below the  ${}^2E$  levels. If, as is observed here, the emission wavelength is relatively close to the absorption, the chromium ions will be only slightly perturbed, and the emission will be quite characteristic of these ions. In particular the emission should yield information about the exchange splittings of the ground state.

Wickersheim<sup>3</sup> has observed the absorption from the  $S_z = -\frac{1}{2}$  excited level of the ground state. It is displaced  $245 \pm 20 \text{ cm}^{-1}$  to the long-wavelength side of the lowest-energy, low-temperature absorption line, and was only observed above  $100^\circ\text{K}$ . The two emission spectra of Fig. 8 show emission in bands at, respectively,  $248$  and  $252 \text{ cm}^{-1}$  from the sharp line. In each case the sharp line and its associated band are thought to originate from the same trap level. For the Verneuil grown crystal, the emission intensity from the  $0$ – $248$ - $\text{cm}^{-1}$  pair decreases with increasing temperature, but the intensity of another pair, at  $535$ – $784 \text{ cm}^{-1}$  from the line labeled  $0$ , increases. Since the energy separation between the latter pair is  $249 \text{ cm}^{-1}$ , this emission is thought to originate from a different trap level. A similar effect was observed for the emission lines labeled

<sup>25</sup> W. Kaiser, S. Sugano, and D. L. Wood, *Phys. Rev. Letters* **6**, 605 (1961); M. D. Sturge, *Phys. Rev.* **133**, A795 (1964).

<sup>26</sup> J. O. Artman and J. C. Murphy, *J. Chem. Phys.* **38**, 1544 (1963); in *Proceedings of the First Conference on Paramagnetic Resonance, Jerusalem, 1962*, edited by W. Low (Academic Press Inc., New York, 1963), Vol. II, p. 634; M. G. Cohen and N. Bloembergen, *Phys. Rev.* **135**, A950 (1964).

<sup>27</sup> E. Royce and N. Bloembergen, *Phys. Rev.* **131**, 1912 (1963).

<sup>28</sup> R. E. Dietz, L. F. Johnson, and H. J. Guggenheim, *Physics of Quantum Electronics*, edited by P. L. Kelley, B. Lax, and P. E. Tannenwald (McGraw-Hill Book Company, Inc., New York, 1966), p. 361.

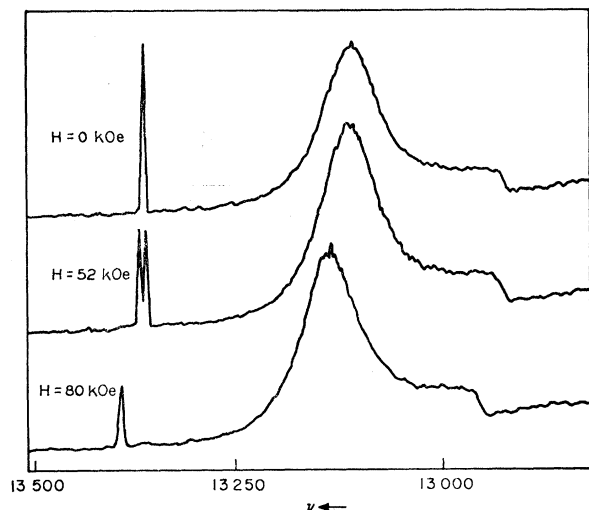


FIG. 9. Fluorescence from the flux-grown crystal with the magnetic field parallel to the  $c$  axis. Above the spin-flop field of 58 kOe, the spectrum shifts to higher energy by  $25\text{ cm}^{-1}$ .

$701$  and  $955\text{ cm}^{-1}$  in the flux-grown crystal. Each type of impurity perturbs the excited states of the chromium ions in its own way, producing trap levels at various energies, but does not appear to appreciably affect the energy separation of the terminating levels of the fluorescence. The temperature dependence of the fluorescence indicates the existence of interesting thermalization processes between various traps present in the same crystal.

We have not been able to identify the specific impurities causing the traps. Analysis of the Verneuil-grown crystal showed it contained 0.1% Al, 0.01% Mg, and traces of transition metal ions other than chromium.

Additional evidence that the fluorescence is closely associated with the chromium ions is obtained from the field dependence of the emission. As shown in Fig. 9

for the flux-grown crystal, in the low-field region the sharp line splits linearly with the field, but the broad band is field-independent. The high-field Bitter magnet was used for the experiment. The spectrum uniformly shifts by  $25\text{ cm}^{-1}$  to shorter wavelengths and the splitting of the sharp line disappears when the field is increased beyond its spin-flop value of 58 kOe. Similarly in absorption, the  ${}^2E$  lines shift and the splitting disappears. These results enable us to identify the sharp line as terminating on the chromium-ion ground state and the band separated by about  $250\text{ cm}^{-1}$  as terminating on the first excited ground-state level. In terms of the exciton description, the latter is termed the *magnon sideband* of the sharp line. In this emission process, a filled trap is emptied, and a spin wave is excited. Magnon sidebands have previously been found in the absorption and emission spectrum of  $\text{MnF}_2$ .<sup>29,30</sup> It should be observed that the characteristics of the emission sidebands are similar for both materials, however in contrast to  $\text{MnF}_2$ , a magnon sideband is not observed in the absorption spectrum of  $\text{Cr}_2\text{O}_3$ .

#### ACKNOWLEDGMENTS

The author wishes to acknowledge several discussions with M. D. Sturge, G. F. Imbusch, and C. G. B. Garrett during the general course of this work and also a discussion with R. E. Dietz concerning the fluorescence data. The Verneuil-grown crystals were grown by R. A. Lefever of the Sandia Corporation, and the flux-grown crystals were prepared here by H. J. Guggenheim. The technical assistance of K. A. Ingersoll and C. R. Staton is appreciated. H. W. Dail gave valuable assistance in the operation of the Bitter magnet.

<sup>29</sup> R. L. Greene, D. D. Sell, W. M. Yen, A. L. Schawlow, and R. M. White, *Phys. Rev. Letters* **15**, 656 (1965).

<sup>30</sup> R. L. Greene, D. D. Sell, and R. M. White, report presented at the Conference on the Optical Properties of Ions in Crystals, Baltimore, Maryland, 1966 (unpublished); D. D. Sell, R. L. Greene, W. M. Yen, A. L. Schawlow, and R. M. White, *J. Appl. Phys.* **37**, 1229 (1966).